



**HAL**  
open science

# Mechanical role of the submembrane spectrin scaffold in red blood cells and neurons

Christophe Leterrier, Pramod A Pullarkat

► **To cite this version:**

Christophe Leterrier, Pramod A Pullarkat. Mechanical role of the submembrane spectrin scaffold in red blood cells and neurons. *Journal of Cell Science*, 2022, 135, 10.1242/jcs.259356 . hal-03759935

**HAL Id: hal-03759935**

**<https://hal.science/hal-03759935v1>**

Submitted on 25 Oct 2022

**HAL** is a multi-disciplinary open access archive for the deposit and dissemination of scientific research documents, whether they are published or not. The documents may come from teaching and research institutions in France or abroad, or from public or private research centers.

L'archive ouverte pluridisciplinaire **HAL**, est destinée au dépôt et à la diffusion de documents scientifiques de niveau recherche, publiés ou non, émanant des établissements d'enseignement et de recherche français ou étrangers, des laboratoires publics ou privés.

## REVIEW

## SUBJECT COLLECTION: CYTOSKELETON

# Mechanical role of the submembrane spectrin scaffold in red blood cells and neurons

Christophe Leterrier<sup>1</sup> and Pramod A. Pullarkat<sup>2,\*</sup>

## ABSTRACT

Spectrins are large, evolutionarily well-conserved proteins that form highly organized scaffolds on the inner surface of eukaryotic cells. Their organization in different cell types or cellular compartments helps cells withstand mechanical challenges with unique strategies depending on the cell type. This Review discusses our understanding of the mechanical properties of spectrins, their very distinct organization in red blood cells and neurons as two examples, and the contribution of the scaffolds they form to the mechanical properties of these cells.

**KEY WORDS:** Red blood cell elasticity, Axonal cytoskeleton, Cell mechanics, Membrane-associated periodic skeleton, Spectrin scaffold

## Introduction

The mechanical properties of cellular scaffolds derive from the integration of properties at several scales, from amino-acid-level flexibility to whole-cell assemblies. Spectrins, thought to have evolved in early unicellular organisms and conserved in metazoans, form distinct scaffolds in differentiated cells, such as epithelial cells, muscle cells, erythrocytes (red blood cells; RBCs) and neurons, and this endows them with unique mechanical properties (Baines, 2009). Following a bottom-up approach, we summarize what is known about the protein structure of spectrins, their macromolecular organization and their integration in cellular scaffolds, highlighting the mechanical implications of each organization level, and detailing how their interplay is reflected when probing the mechanical behavior of RBCs and the axons of neurons. This comparison will delineate recent insights and open questions about the mechanical role of the submembrane spectrin scaffold.

## Spectrin structure

### Spectrin subunits

Spectrin was originally discovered by Marchesi and Steers as a component of the RBC membrane from ghosts preparations, hence its name coming from ‘specter’ (Marchesi and Steers, 1968). They isolated the erythrocyte-specific spectrin tetramer comprising  $\alpha$ 1- and  $\beta$ 1-spectrin (encoded by *SPTA1* and *SPTB*, respectively, in humans). Spectrin is a constitutive component of the RBC submembrane scaffold, where it associates with ankyrin-R (also known as ANK1), band 4.1R (also known as EPB41) and short actin filaments (Winkelmann and Forget, 1993). Biochemical studies have shown that the  $\alpha$ - and  $\beta$ -subunits of spectrin associate as

antiparallel  $\alpha\beta$  dimer, then as a head-to-head ( $\alpha\beta$ )<sub>2</sub> tetramer. Furthermore, early electron microscopy (EM) studies of purified spectrin revealed that spectrin dimers and tetramers adopted a 200 nm elongated shape (Cohen et al., 1980; Shotton et al., 1979).

In the early 1980s, radiolabeling experiments revealed a spectrin-like protein among the slow axonal transport cargoes (Levine and Willard, 1981). Development of specific antibodies allowed the identification of non-erythrocyte spectrin in multiple cell types, including neurons (Burrige et al., 1982; Goodman et al., 1981; Repasky et al., 1982). This non-erythrocyte spectrin, also named fodrin, is made of  $\alpha$ 2- and  $\beta$ 2-spectrin (encoded by *SPTAN1* and *SPTBN1*, respectively, in humans) and also adopts a 200 nm long rod shape when observed by EM (Bennett et al., 1982; Glenney et al., 1982). Whereas  $\alpha$ 1-expression is mostly restricted to erythrocytes where it combines with  $\beta$ 1-spectrin,  $\alpha$ 2- and  $\beta$ 2-spectrin are more ubiquitous. More  $\beta$ -spectrin subunits were subsequently discovered, and named  $\beta$ 3- (encoded by *SPTBN2*) (Ohara et al., 1998),  $\beta$ 4- (*SPTBN4*) (Berghs et al., 2000) and  $\beta$ 5-spectrin (*SPTBN5*) (Stabach and Morrow, 2000), with  $\beta$ 3- and  $\beta$ 4-spectrins also expressed in neurons together with  $\alpha$ 2-spectrin. In addition, shorter isoforms of various  $\beta$ -spectrin have been described (Bennett and Baines, 2001).

At the end of the 1980s, when spectrin amino acid sequences were determined, starting with  $\alpha$ 2-spectrin (Wasenius et al., 1989), the arrangement of the spectrin domains and the structure of the tetramers were already well known. The core structural feature of spectrin subunits are spectrin repeats, domains of 106 amino-acids (~12 kDa) that form three helices connected by loops (Fig. 1A) (Kusunoki et al., 2004; Speicher and Marchesi, 1984). The assembled spectrin repeat is stable, with flexibility between repeats (DeSilva et al., 1997; Grum et al., 1999). Erythrocyte and non-erythrocyte spectrins have a similar organization (Sreeja et al., 2020) –  $\alpha$ -spectrins have 21 repeats, with repeat 10 being different and connected to a SH3 domain.  $\beta$ -spectrins have 17 repeats, and a pair of calponin-homology domains at the amino-terminus that interacts with actin (Fig. 1B). Dimerization of  $\alpha$ - and  $\beta$ -spectrin occurs by the antiparallel association of repeats 20–21 of  $\alpha$ -spectrin with repeats 1–2 of  $\beta$ -spectrin. Formation of the ( $\alpha\beta$ )<sub>2</sub> tetramer occurs by head-to-head association of two dimers, involving the first repeats of  $\alpha$ -spectrin and the final ones (16–17) of  $\beta$ -spectrin (Fig. 1C).

### Conformations of spectrin tetramers

The assembled spectrin tetramer was initially assessed to be ~200 nm long for purified tetramers by electron microscopy. However, this contour length is inconsistent with the 70 to 80 nm length estimated from the number of spectrin tetramers, their hexagonal organization, and the overall surface of RBCs (see below) (Lux, 2016). Moreover, visualization of spectrin tetramers *in situ* using EM yielded lengths of between 50 and 200 nm depending on the exact technique used, whereas more recent

<sup>1</sup>Aix Marseille Université, CNRS, INP UMR 7051, NeuroCyto, Marseille 13005, France. <sup>2</sup>Raman Research Institute, Bangalore 560 080, India.

\*Author for correspondence (pramod@rri.res.in)

© C.L., 0000-0002-2957-2032; P.A.P., 0000-0003-2716-7575

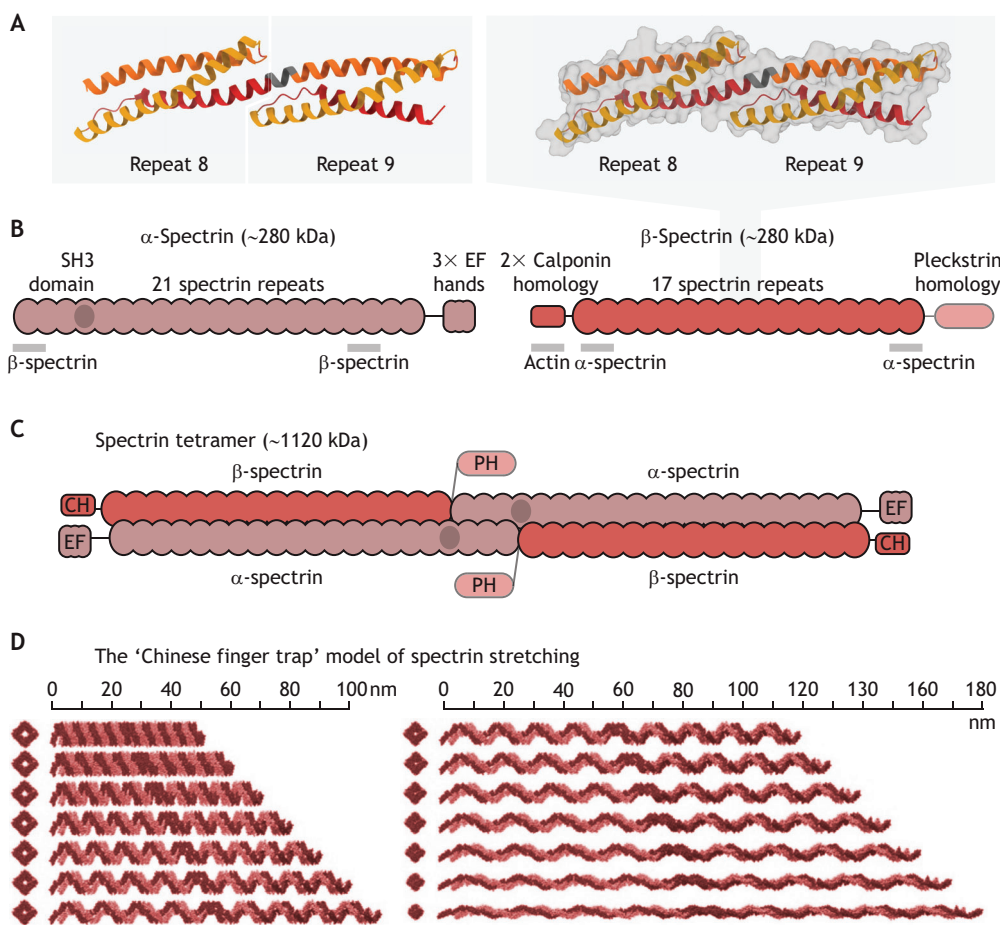


**Fig. 1. The spectrin tetramer structure.** (A) Molecular structure of two spectrin repeats (repeats 8 and 9 of human  $\beta$ 1-spectrin; PDB 1S35; Kusunoki et al., 2004), showing the three helices in each repeat (left) and the corresponding surface (right). (B) Domain organization of  $\alpha$ - (left) and  $\beta$ -spectrins. The pleckstrin homology (PH) domain of  $\beta$ -spectrins is absent from  $\beta$ 1-spectrin. Regions of interaction between subunits and with partners are highlighted below each subunit. (C) Organization of the head-to-head assembled spectrin tetramer. (D) 'Chinese finger trap' model of spectrin stretching showing how the tetramer can measure between 50 and 180 nm [adapted from Brown et al. (2015) where it was published under a CC-BY 4.0 license].

super-resolution microscopy data found an average length of  $\sim 70$  nm (Pan et al., 2018). These discrepancies suggest that the spectrin tetramer is able to adopt a range of higher-order structures that would be differently affected by the purification and sample preparation process.

Fourier analysis of electron micrographs obtained from partially expanded tetramers has revealed that the  $\alpha$ - and  $\beta$ -spectrins coil around each other in the form of a two-start helix, forming a higher-order structure (McGough and Josephs, 1990). Measuring the helix pitch and diameter, and correlating them with the contour lengths, has led to the conclusion that the tetramer can exist with varying degrees of condensation. The native tetramer is thus expected to have a pitch of 7 nm (roughly four residues) and a diameter of 5.9 nm, resulting in the short length of  $\sim 70$  nm observed in some EM studies.

Recently, a new model has been proposed for spectrin tetramers where  $\alpha$ - and  $\beta$ -spectrin repeats coil around each other by forming  $90^\circ$  bends between adjacent repeats (Brown et al., 2015). Although the repeats are linked through continuous helices in the extended conformation (Fig. 1A), it is hypothesized that twist deformation can concentrate within a few inter-repeat  $\alpha$ -helix residues by forming a pi-helix. This leads to a supercoiling of each spectrin strand within the tetramer complex, resulting in a tubular structure with the two sets of repeats wrapped around the tube surface (Fig. 1D). This superstructure model agrees with the diameter of purified spectrin tetramers measured using cryo-EM. This 'Chinese finger trap' model proposed by Brown et al. gives a length of  $\sim 55$ – $65$  nm for the 'native state' of the tetramer, close to the range observed in the super-resolution images of RBCs (Pan et al., 2018).

According to this model, a forced extension of the contour length of the tetramer superstructure will result in a corresponding decrease in diameter, as observed previously (McGough and Josephs, 1990), until it reaches the fully extended conformation (Fig. 1D). Further stretching of the fully extended form can lead to unfolding of the triple  $\alpha$ -helix repeats. Such responses have been extensively investigated at the single-protein level and the main findings are summarized in the next section.

### Mechanical properties of single spectrins – repeats unfolding and tetramer extension

#### Mechanical properties of spectrin repeats

The formation of submembrane scaffolds by spectrins, the striking variability of the tetramer length, and the nature of their secondary and tertiary structure has led to a lot of interest in the mechanical properties of single spectrins. Here we must distinguish the mechanical properties of repeats themselves, which has been extensively studied, and the properties of the assembled tetramers, which are more difficult to assess. Atomic force microscopy (AFM) experiments conducted on five recombinant repeats of chicken brain spectrin and the full purified human erythrocyte spectrin has revealed that these show sequential unfolding events (Rief et al., 1999). The triple  $\alpha$ -helix of spectrin repeats unfolded at forces of  $\Delta F$  of  $\sim 25$ – $35$  pN when pulled at  $0.3 \mu\text{m/s}$  (Fig. 2A). Each unfolding added 31.7 nm in length which corresponds to  $\sim 106$  amino acid residues, indicating complete, single-step unfolding of the triple helix repeat. The resulting sawtooth shaped force response (Fig. 2B) could be reproduced under stretch-recovery cycles showing that the unfolding process is reversible (Rief et al., 1999).

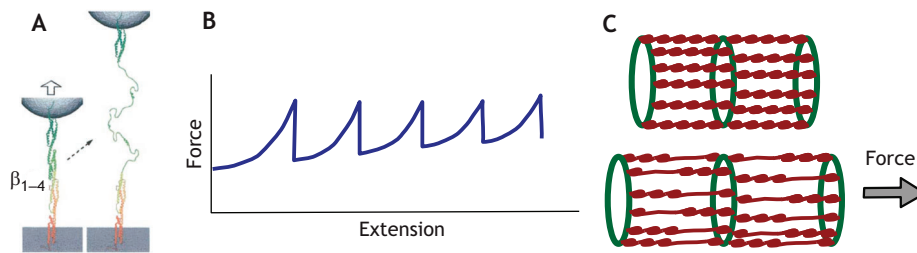


**Fig. 2. Unfolding of the spectrin repeats.** (A) Schematic illustration of force-induced unfolding of spectrin repeats in an AFM experiment. Adapted with permission from Law et al. (2003) with permission from Elsevier. (B) Schematic illustration of a typical force–extension curve showing saw-tooth like events, each force drop corresponding to a single repeat unfolding. Also note the non-linear increase between unfolding events, which is characteristic of semi-flexible polymers (Rief et al., 1999). (C) Schematics showing the possible unfolding of spectrin repeats connecting the actin rings of an axon when the axon is subjected to a stretching force.

The energy needed for spectrin repeat unfolding can be estimated from the force–extension data and is of the order of  $\Delta E = \Delta F \cdot \Delta x \sim 4 \times 10^{-21}$  J (where  $\Delta x$  is the distance between the folded and unfolded state minima). This energy barrier is of the same order of magnitude as the typical thermal energy at physiological temperatures, which is given by  $k_B T$ , where  $k_B$  is the Boltzmann constant and  $T$  the absolute temperature. Therefore, the unfolding–refolding process is stochastic, and thermally assisted unfolding can happen. When an external force is applied, the lifetime of the folded state is expected to decrease with increasing force, as described by the Bell model,  $\tau = \tau_0 e^{-\Delta F \cdot \Delta x / k_B T}$ , where  $\tau_0$  is the lifetime in the absence of force (Bell, 1978; Evans and Ritchie, 1997). As demonstrated by the experiments noted above (Rief et al., 1999), the stochastic nature of this process makes the unfolding process sensitive to the rate at which the external force is applied. In addition, their AFM data also show that in a given folded or unfolded state, spectrin exhibits elastic properties similar to that of a semiflexible polymer (Box 1). This is further supported by direct observations of ‘worm-like’ conformations of spectrin in electron micrographs (Shotton et al., 1979). Semiflexible polymers undergo significant thermal fluctuations and resist any deformation that decreases this fluctuation. This leads to a temperature-dependent entropic elasticity, where the force increases with extension in a highly non-linear fashion (Fig. 2B; Box 1).

### Box 1. Entropic elasticity of polymers

When the two ends of a semi-flexible polymer are pulled apart by applying an external force, the resulting force versus extension ( $F$  vs  $x$ ) behavior is well described by the worm-like chain model (WLC model) (Bustamante et al., 1994):

$$F(x) = \frac{k_B T}{l_p} \left[ \frac{1}{4} \left( 1 - \frac{x}{L_c} \right)^{-2} - \frac{1}{4} + \frac{x}{L_c} \right], \quad (1)$$

for  $x < L_c$ , where  $l_p$  is the persistence length, which is a measure of the flexibility of the backbone to bending (the more flexible the polymer, the lower its persistence length), and  $L_c$  is the contour length of the protein. In the case of spectrin,  $L_c$  increases by  $\sim 30$  nm ( $\sim 106$  residues) when each repeat unfolds (Rief et al., 1999). Only indirect measurements of the persistence length are available, giving a range of  $\sim 1$ – $20$  nm depending on the technique used (Rief et al., 1999; Shotton et al., 1979; Stokke et al., 1985). For comparison, a single-stranded DNA has a persistence length of  $\sim 1$  nm and it reaches 50 nm for double-stranded DNA. The combined effects of the WLC response and the ability of repeats to unfold gives rise to the kind of force response observed (Rief et al., 1999), which is schematically shown in Fig. 2B.

Subsequent AFM experiments using short recombinant constructs have further revealed cooperative unfolding of adjacent spectrin repeats (Law et al., 2003). The cooperativity is thought to arise due to the continuity of the linker helix between the repeats (Fig. 1A). AFM-based force spectroscopy of repeat pairs connected with native helical or immunoglobulin-based non-helical linkers have shown no cooperative unfolding between repeats connected by non-helical linkers, whereas rare cooperative unbinding events were observed in repeats with native helical linkers (Randles et al., 2007). Computer simulation supports a role for the linker structure in the unfolding behavior of adjacent repeats (Ortiz et al., 2005). Irrespective of the details of the unfolding process, a large body of experimental and modeling studies support the idea that the repeats of spectrin molecules can easily unfold under stretch and refold when relaxed. However, how the assembled tetramers might behave when stretched is still an open question.

### Mechanical properties of spectrin tetramers

Beyond the unfolding within spectrin repeats, a more complete understanding of the contribution of the spectrins to cell mechanics is necessary to understand the dynamics and mechanical response of fully assembled spectrin tetramers. Going by the proposed Chinese finger trap model (Fig. 1D), one may assume that the weak lateral interactions between the repeats in the hollow-tube configuration could be easily disrupted under mechanical perturbations. Given that purification of structurally intact tetramers can be challenging, alternate methods such as *in situ* cryo-EM of tetramer configuration in normal and mechanically stressed cells could be used to shed some light on this problem. Recently, fluorescence resonance energy transfer (FRET)-based molecular tension sensors have been successfully used to show that neuronal spectrins are held under tension (Krieg et al., 2014). The quantitative nature of FRET measurements makes it an attractive method to investigate the relationship between tension versus extension responses of spectrin tetramers.

### The spectrin-based scaffold in RBCs

Moving up from the molecular arrangement and mechanics of isolated spectrin repeats and individual tetramers, we now turn to the role of spectrin scaffold in RBCs and the axon of neurons. Below, we first discuss the organization of this skeleton in RBCs and our current understanding of its mechanical relevance.

### The architecture of the submembrane spectrin scaffold in RBCs

Compared to other eukaryotic cells, the structural organization of mature erythrocytes is extremely simple. In most mammals (some ungulates, like camels, are exceptions), mature RBCs

have a biconcave shape and are devoid of both a nucleus and microtubules – the inside of erythrocytes is free of any organized cytoskeletal structures, except for the membrane-associated actin–spectrin scaffold. Thus, the mechanical properties of RBCs are dictated by the outer composite layer, which is composed of a lipid bilayer membrane and an attached layer of actin–spectrin meshwork (Fig. 3A) (Fowler, 2013).

This simple organization allowed for the discovery of spectrin in erythrocytes more than 50 years ago (Marchesi and Steers, 1968), quickly followed by the identification of short, capped actin filaments attached at the network nodes and other spectrin partners, such as ankyrin and membrane proteins. The arrangement of the spectrin mesh along erythrocyte membrane was investigated by various EM techniques, first revealing an irregular end-to-end meshwork (Tsukita et al., 1981), resolved to be a pseudo-hexagonal mesh of spectrin tetramers on spread erythrocyte membranes (Byers and Branton, 1985; Liu et al., 1987). These studies visualized stretched spectrin tetramers to their full 200 nm length (Fig. 3B), but the meshwork from fixed native erythrocytes had much shorter 30–50 nm branches that were obscured by the density of proteins (Ohno, 1992), with segmentation of cryo-electron tomography data measuring tetramers of ~50 nm in length (Nans et al., 2011). The Chinese finger trap model (see above) could explain how spectrin is able to change its length between 50 and 200 nm, but more disordered ‘worm-like’ conformations have also been proposed for the spectrin tetramers in resting erythrocytes (Gokhin and Fowler, 2016). Assuming a homogenous network, a simple calculation from the number of spectrin filaments and the surface of an erythrocyte would result in a tetramer length of 70 to 80 nm. Recently, super-resolution optical microscopy of the resting erythrocyte membrane was able to measure a 70-nm length, consistent with this estimation (Fig. 3C,D; Pan et al., 2018). The capacity of spectrin to stretch or compress from this average value is likely key to RBC function as these cells undergo large and repeated cycles of deformation as they squeeze through micro-capillaries.

#### Mechanical role of the spectrin-based scaffold in RBCs

The elastic properties of the lipid bilayer membrane alone is sufficient to account for biconcave shapes in synthetic vesicles (Box 2) (Canham, 1970; Seifert, 1997). However, the spectrin sublayer has a crucial role in imparting shape stability to RBCs.

Several genetic disorders caused by spectrin mutations, such as elliptocytosis, result in loss of RBC shape, and expressing normal spectrin can lead to recovery of the shape, suggesting a significant role for spectrin in imparting shape stability to RBCs (Agre et al., 1985; Costa et al., 2020; Mohandas and Evans, 1994; Tomaiuolo, 2014). Unlike the membrane, which cannot resist in-plane shear deformations, the spectrin scaffold can provide solid-like shear elasticity at timescales shorter than any structural remodeling time. Moreover, differential tension can exist between the lipid and the spectrin layers (one can be under stretch while the other is under compression), which then generates curvature. Finally, as will be elaborated later, the ability of spectrin to undergo reversible unfolding or unbinding influences the mechanical response of cells to stretch deformations. Several theoretical models incorporating one or more of these properties have been developed to describe how spectrin stabilizes the discoidal shape of RBCs and under what conditions abnormal shapes can appear (Canham, 1970; Elgsaeter et al., 1986; Geekiyanage et al., 2019).

Apart from this shape stabilizing role, the submembrane spectrin scaffold plays a critical role in protecting RBCs as they undergo large deformations when they squeeze through capillaries narrower than their diameter (Li et al., 2018; Tomaiuolo, 2014). Blood flow in larger vessels also causes significant fluid shear stress on RBCs and altered elastic properties that affect blood fluid dynamics (Dupire et al., 2012). This has generated much interest in understanding the viscoelastic properties of RBCs, which we summarize below.

#### Measurements of RBC mechanics

When a flaccid biconcave RBC is partially aspirated into a glass micropipette of a few microns in diameter, the cell protrudes into the pipette while preserving the cell surface area and the deformation is dominated by shear forces. When osmotically swollen RBCs are used, the elastic response is dominated by membrane stretch. Using these methods, the shear modulus was measured to be 6.6  $\mu\text{N/m}$  and the stretching modulus to be 0.45 N/m at 25°C (Waugh and Evans, 1979). In addition, this study showed that these values decrease with increasing temperature in the range of 2°C to 50°C. More recent optical tweezer based measurements yielded a shear modulus of 2–5  $\mu\text{N/m}$  (Hénon et al., 1999; Mills et al., 2004). Significant softening of the shear modulus with increased deformation was also observed in some of these studies (Mills et al., 2004). (See Kim

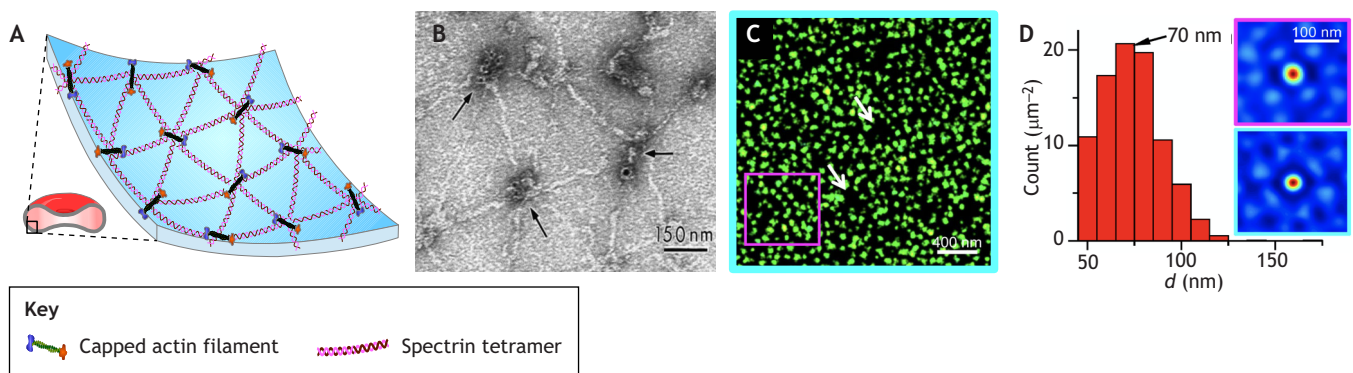


**Fig. 3. The architecture of the submembrane spectrin scaffold in RBCs.** (A) Schematic illustration of the inner surface of a RBC membrane with its actin–spectrin submembrane scaffold. This skeleton has a predominantly hexagonal arrangement of spectrin tetramers linked by short (~60 nm) and capped actin filaments. (B) Early EM experiments revealed the hexagonal arrangement of spectrin tetramers in RBC ghosts. A range of lengths were seen for the spectrin tetramers due to specimen stretch with an upper limit of about 200 nm; adapted from Ursitti and Fowler (1994) with permission. (C) Super-resolution images of the N-terminus of  $\beta$ -spectrin reveal their structure in RBCs with an average inter-nodal distance of 70 nm. (D) Histogram showing the inter-nodal distance distribution, and autocorrelation plots showing the overall hexagonal symmetry. Images in C and D adapted from Pan et al. (2018) where they were published under a CC-BY 4.0 license.

### Box 2. Elastic response of lipid bilayer membranes

A lipid bilayer is a two-dimensional fluid in the plane of the membrane but has interesting elastic properties. It resists in-plane stretching, as this involves changing the area per molecule of the lipid bilayer. It also resists bending. These two are regarded as independent deformations because the membrane can be stretched without bending and bent without stretching (bending involves splaying of molecules). However, being a 2D fluid, it cannot resist in-plane shear deformations. In its simplest form, the elastic free energy per unit area of closed vesicles can be described by the Helfrich–Canham elastic free energy expression

$$F_{\text{memb}} = k_{\text{stretch}} \left( \frac{\Delta a}{a_0} \right)^2 + k_{\text{bend}} C^2 + k_G C_G \text{ (Seifert, 1997)},$$

where  $k_{\text{stretch}}$  is the stretching elastic moduli,  $\Delta a$  is the change in area per molecule with respect to the unstretched (ground state) area  $a_0$ ,  $C$  and  $C_G$  are the mean and Gaussian curvatures of the membrane, and  $k_{\text{bend}}$  and  $k_G$  are the corresponding elastic moduli, respectively. Minimization of this free energy integrated over the closed surface (the Gaussian curvature term yields a constant for a fixed topology, irrespective of shape) gives the preferred shape of the vesicle for a fixed enclosed volume. Interestingly, such membrane elasticity considerations alone show that discoidal shapes are preferred for certain surface to volume ratios (Canham, 1970; Seifert, 1997).

et al., 2015 for a review of the various techniques for measuring these mechanical properties).

Several experiments have indicated that RBCs exhibit non-linear elastic responses (Lee and Discher, 2001; Mills et al., 2004). In particular, analyzing the mean square fluctuation of nanoparticles tethered to actin at spectrin mesh nodes has shown that the network softens with imposed deformation (Lee and Discher, 2001). This, along with the earlier observation that the skeleton softens with increasing temperature (Waugh and Evans, 1979), points towards the possibility of a repeat unfolding mechanism playing a significant role in defining the RBC viscoelastic response. This is because the entropic elasticity alone described by the worm-like chain (WLC) model (Box 1) predicts stiffening with increasing temperature. Softening of the spectrin skeleton could also occur if the network integrity is lost under deformation, for example via detachment of the actin-spectrin linkages or  $\alpha\beta$  spectrin contacts (An et al., 2002; Gov, 2007; Lee and Discher, 2001).

Significant evidence for force-induced unfolding comes from experiments that quantify the stress-induced exposure of otherwise hidden cysteine residues within the folded repeats of  $\alpha$ - and  $\beta$ -spectrins (Johnson et al., 2007). The exposure of hidden cysteine residues upon physiologically relevant stress of  $\sim 1$  Pa is detected by loading the cells with cysteine-binding fluorophores and assessing the increased fluorescence of extracts from these cells on SDS-PAGE gels, followed by digestion and mass spectrometry to localize the exposed cysteine residues. Sheared cells showed 50% more fluorescence, and mass spectrometry revealed exposed cysteines within the triple helix repeats, suggesting unfolding of the repeats under stress. In a subsequent study, cells with a 4.1R mutant showed markedly reduced labeling in sheared cells possibly due to easy detachment of spectrins from actin nodes (Krieger et al., 2011).

In addition to these mechanical aspects, the presence of capped, but possibly dynamic, actin filaments (Gokhin et al., 2015), ATP-dependent membrane properties (Betz et al., 2009) and myosin contractility within the RBC spectrin scaffold (Smith et al., 2018) makes this skeleton dynamic, with possible consequences for its viscoelastic properties that we have not detailed here. Based on observation of dynamic ‘actin foci’, it has recently been proposed that spectrin spacing might be heterogeneous and fluctuating

throughout the RBC (Nowak et al., 2022). A large body of work has thus been dedicated to investigating forced unfolding of single spectrins, the whole-cell mechanical response and, to some extent, the active dynamics of the actin-spectrin scaffold in RBCs. The interplay of these processes is still unclear, however, as is the *in-situ* contribution of spectrin length change via conformation change in the proposed Chinese finger trap structure between compacted and fully extended states (Fig. 1D).

### The spectrin-based scaffold in neurons

#### The architecture of the submembrane spectrin scaffold in axons

Neurons express a larger repertoire of spectrins including  $\beta 1$  and  $\alpha 2$ – $\beta 2$ , as well as  $\beta 3$  and  $\beta 4$  spectrins (Lorenzo, 2020). In the axon, tetramers of  $\alpha 2$ – $\beta 4$  are present along the axon initial segment, whereas the more distal axon mostly contains  $\alpha 2$ – $\beta 2$  tetramers (Liu and Rasband, 2019). The submembrane arrangement of axonal spectrins was revealed in 2013 by super-resolution microscopy (Xu et al., 2013) – fully extended spectrin tetramers connecting actin rings spaced 190 nm apart form a submembrane-periodic scaffold (Fig. 4). This structure seems to be ubiquitous, as it has been observed in all mature neurons across several species (D’Este et al., 2016; He et al., 2016). The cytoskeleton of neurites also includes longitudinally aligned microtubules, neurofilaments and actin filaments that are not part of the ring system, and a large variety of crosslinking proteins and motor proteins (Fig. 4A) (Kevenaar and Hoogenraad, 2015; Leterrier, 2021; Leterrier et al., 2017; Prokop, 2020). Unlike in RBCs, the composite cytoskeletal organization in neurons and the interdependencies between the different elements makes delineating specific contributions to axonal stability more challenging (Qu et al., 2017). Below, we discuss recent studies that focus on the mechanical role of the periodic actin–spectrin scaffold in axons.

#### Mechanical role of the spectrin-based scaffold in axons

The 190 nm spacing of the periodic spectrin scaffold along axons suggests that the tetramers are in the fully extended conformation, even in the absence of imposed deformation. Whether the tetramers assemble in the fully extended configuration or whether they get stretched to this state post-assembly is not clear, and the significance of this structure to axon mechanics is only beginning to emerge. A clear indication of a mechanical role for the spectrin scaffold in axons came from the observation that axons of *C. elegans* lacking  $\beta 2$ -spectrin snap under stresses generated by normal wiggling of the worm (Hammarlund et al., 2007). Subsequent studies using a FRET-based tension sensor incorporated into  $\beta 2$ -spectrin of worms showed that the axonal spectrin is held under tension and this tension is released when axons are transected using a laser (Krieg et al., 2014).

Recent measurements of the axonal mechanical response using chick dorsal root ganglia neurons and an optical-fiber-based technique revealed that disruption of actin rings or knockdown of  $\beta 2$ -spectrin leads to a substantial reduction in the axonal elastic modulus (Dubey et al., 2020). In addition, this study showed that the axonal Young’s modulus decreases with increasing strain (strain-softening response), unlike most other cell types and biopolymer networks where it increases with strain or stress (Pullarkat et al., 2007; Storm et al., 2005). A theoretical model, which describes the spectrin tetramer as a WLC containing tandem repeats that can reversibly unfold in a tension-dependent manner, captured the strain softening as well as the non-monotonous behavior of the stress relaxation time with imposed strain seen in axon experiments (Dubey et al., 2020). The rest tension in unstretched axons in culture is only a few nanonewtons. A simple estimate gives an axonal

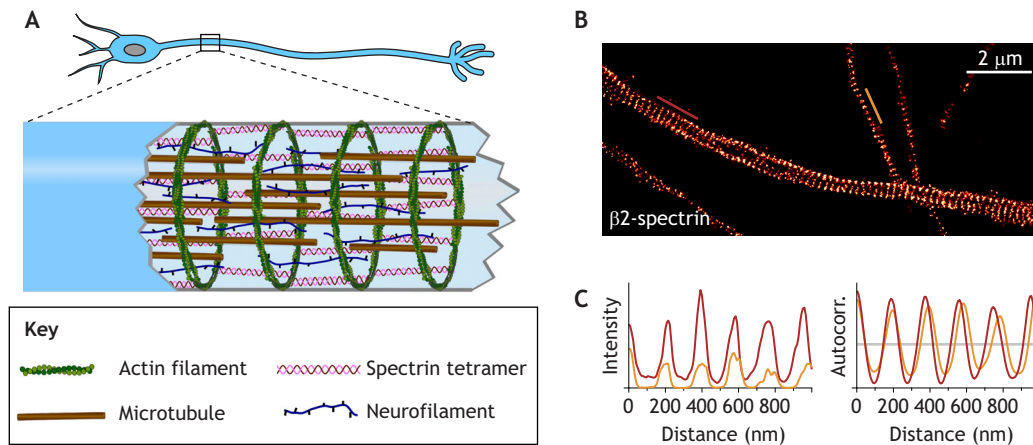


**Fig. 4. The architecture of the submembrane spectrin scaffold in axons.** (A) Schematic illustration of the organization of the axonal cytoskeleton. The outermost layer consists of periodically spaced rings of actin filaments with a spacing of about 190 nm. The rings are interconnected by spectrin tetramers. The interior has bundles of microtubules which are crosslinked by microtubule associated proteins. Neurofilaments, neuronal analogs of intermediate filaments, also fill the interior of the axon. (B) A 2D STORM image of  $\beta$ 2-spectrin in axons. (C) Intensity (left) and autocorrelation (right) for line profiles drawn in B.

tension of 6–10 nN before unfolding might happen. Such tensions are easily reached when axons in culture are suddenly stretched by a strain of 5 to 10% (Dubey et al., 2020). It is conceivable that, at low rest tensions, axonal spectrins exist in the fully extended form and that beyond a higher threshold value, reversible unfolding might ensue. It is also possible that spectrins might dissociate under tension, although the  $\alpha$ 2– $\beta$ 2 neuronal spectrin association is much stronger than in the RBC counterparts (An et al., 2002, 2006). The possibility of reversible unfolding or unbinding needs to be explored through future experiments. Overall, these results suggest that the axonal spectrin skeleton can act as a tension buffer by unfolding spectrin repeats when subjected to mechanical stress (Fig. 2C).

AFM data based on local indentation of the axonal membrane followed by coarse-grained molecular dynamics simulations also suggest that the spectrin scaffold significantly influences membrane mechanics and that damage to this skeleton can compromise axonal integrity under injury-causing conditions (Zhang et al., 2017). A recent computational analysis of the composite axon further highlights the role of the spectrin scaffold, along with other elements, under concussion or traumatic brain injury-causing conditions (Kant et al., 2021). As long axons are subjected to large deformations during body movements, especially at the joints, or during head impacts, spectrin-based tension buffering mechanisms might have evolved to offer some protection against stretch-induced damage to axons. However, mechanical stress resistance is not the whole story. The spectrin scaffold is likely to support the neuronal architecture beyond its role in resisting stretch-induced damage, as depletion of  $\alpha$ 2-spectrin results in widespread degeneration of axons in the brain, which are not subjected to large-scale mechanical stress (Huang et al., 2017a). This process preferentially affects large diameter axons of peripheral nervous system (PNS) nerves, where both small and large axons are subject to similar stress (Huang et al., 2017b).

#### Contribution of the actin-spectrin scaffold to axonal caliber and contractility

In addition to its contribution to axonal response to stretch deformations, the actin–spectrin scaffold also appears to play a role in regulating the axonal caliber (Costa et al., 2020; Leite et al., 2016). The mechanics of this scaffold might also be important in facilitating axonal transport (Wang et al., 2020). The relative organization of the myosin-II mini-filaments associated with the

actin rings suggest that myosin-II-driven contractility of the rings might play an important role. Axons are also known to generate longitudinal tension driven by actomyosin activity, and the possible role of the actin–spectrin skeleton in this is still unclear (Mutalik et al., 2018; Rajagopalan et al., 2010). It is possible that part of this tension is also stored passively in the spectrin scaffold as the tetramers exist in a fully extended state. Indeed, FRET measurements and laser ablation studies provide credence to such a view (Krieg et al., 2014). How exactly myosin heads can generate circumferential or longitudinal tension by acting on adjacent rings is still an open question, although some mechanisms have been postulated (Pan et al., 2021).

#### Organization in soma

Although we focus on the periodic spectrin scaffold along axons, spectrin is also present in other neuronal compartments, such as the dendrites and the cell body, and the organization in these compartments raises further intriguing questions. Investigation of the spectrin scaffold in the neuronal cell body revealed a RBC-like pseudo-hexagonal organization in significant sections, although this had an average spacing of  $\sim$ 190 nm (Han et al., 2017). Some dendritic regions show a periodic, unidimensional organization, but remarkably, a few regions of the dendrites also show a two-dimensional (2D) pseudo-hexagonal organization. These observations raise a number of questions. Could the spatial organization depend on the geometry of the surface – a thin cylinder with high curvature versus the cell surface with a much lower curvature? We note that some of the dendrites had diameters significantly larger than an axon (up to 2.6  $\mu$ m; Han et al., 2017). Moreover, one-dimensional (1D) periodic spectrin scaffold has been reported in neuronal cilia, which are also thin cellular extensions (Jia et al., 2019). However, 1D periodic patterns of spectrin can appear also along a flat membrane, as a recent study showed 180-nm spaced bands of spectrins in sheet-like areas of the undifferentiated neuronal stem tissue (Hauser et al., 2018). Second, is the fully extended spectrin length of  $\sim$ 190 nm (compared to  $\sim$ 70 nm for RBCs) due to the soma being in a state of mechanical tension, or is this influenced by biochemical factors alone? More generally, why are neuronal spectrin spread to 190 nm in both 2D hexagonal and 1D longitudinal arrangements, whereas erythrocyte spectrins form a 2D meshwork with a much shorter arrangement of spectrins? Further experiments are required to answer these interesting questions.

## Conclusions and future directions

In this Review, we summarized the knowledge and open questions about mechanical functions of the spectrin scaffold, with applications to the physiology of RBCs and neurons. Spectrins have several other important roles in these cells, signaling being a prime example (Machnicka et al., 2014), which was recently shown to be regulated by the periodic actin-spectrin scaffold along axons (Zhou et al., 2019). Organized distribution of spectrin is also found in other cell types, such as within the stereocilia of inner ear cells, with implications for hearing (Liu et al., 2019). Several other differentiated cells, such as epithelial cells and muscle cells, have extensive spectrin scaffolds but its detailed organization is less clear. Finally, we did not discuss the physiopathological relevance of spectrin mutations beyond erythrocyte spectrins, with spectrin mutations leading to spectrinopathies affecting neurons and brain development (Cousin et al., 2021; Liu and Rasband, 2019), as well as reduced touch sensitivity (Krieg et al., 2014).

In conclusion, a comparison of the spectrin organization and its mechanical roles in RBCs and neurons suggests that these proteins have evolved to act as molecular shock absorbers by virtue of their ability to stretch via conformational transitions, including unfolding of repeats. This is akin to other structural proteins, like for example, the muscle protein titin (Kellermayer et al., 1997; Rief et al., 1997) and the focal adhesion complex talin proteins (Yao et al., 2016). As discussed in this Review, the importance of spectrins in providing stability to RBCs as they squeeze through narrow capillaries have been studied in some detail but their protective role and how they influence axonal caliber are only beginning to be understood. Future experiments such as EM of these scaffolds subjected to controlled deformations and FRET-based fluorescence imaging are required to probe the force-induced conformational changes, repeat unfolding and possible dissociation events in a more precise manner.

Finally, how the spectrin-based scaffold assembles into distinct patterns in different cell types or sub-cellular compartments is also not well understood. Comparisons across cell types might help to reveal the interplay between membrane geometry, mechanical stress, biochemical factors and the type of spectrin organization. The respective role of actin and various spectrins within the neuronal periodic scaffold also remains to be clarified, as dendritic spines can contain actin rings but no detectable  $\beta$ 2-spectrin (Bär et al., 2016). Experimental strategies that can disrupt this scaffold in a reversible manner combined with live-cell super-resolution imaging might provide some answers. *In vitro* reconstituted systems could also be a powerful tool for understanding the organizational principles of these fascinating scaffolds.

## Competing interests

The authors declare no competing or financial interests.

## Funding

C.L. acknowledges support through the Agence Nationale de la Recherche (ANR; ANR-20-CE13-0024) and P.A.P. acknowledges support through The Wellcome Trust DBT India Alliance (grant IA/TSG/20/1/600137).

## References

Agre, P., Casella, J. F., Zinkham, W. H., McMillan, C. and Bennett, V. (1985). Partial deficiency of erythrocyte spectrin in hereditary spherocytosis. *Nature* **314**, 380-383. doi:10.1038/314380a0

An, X., Lecomte, M. C., Chasis, J. A., Mohandas, N. and Gratzer, W. (2002). Shear-response of the spectrin dimer-tetramer equilibrium in the red blood cell membrane. *J. Biol. Chem.* **277**, 31796-31800. doi:10.1074/jbc.M204567200

An, X., Guo, X., Zhang, X., Baines, A. J., Debnath, G., Moyo, D., Salomao, M., Bhasin, N., Johnson, C., Discher, D. et al. (2006). Conformational stabilities of the structural repeats of erythroid spectrin and their functional implications. *J. Biol. Chem.* **281**, 10527-10532. doi:10.1074/jbc.M513725200

Baines, A. J. (2009). Evolution of spectrin function in cytoskeletal and membrane networks. *Biochem. Soc. Trans.* **37**, 796-803. doi:10.1042/BST0370796

Bär, J., Kobler, O., van Bommel, B. and Mikhaylova, M. (2016). Periodic F-actin structures shape the neck of dendritic spines. *Sci. Rep.* **6**, 37136. doi:10.1038/srep37136

Bell, G. I. (1978). Models for the specific adhesion of cells to cells. *Science* **200**, 618-627. doi:10.1126/science.347575

Bennett, V. and Baines, A. J. (2001). Spectrin and ankyrin-based pathways: metazoan inventions for integrating cells into tissues. *Physiol. Rev.* **81**, 1353-1392. doi:10.1152/physrev.2001.81.3.1353

Bennett, V., Davis, J. and Fowler, W. E. (1982). Brain spectrin, a membrane-associated protein related in structure and function to erythrocyte spectrin. *Nature* **299**, 126-131. doi:10.1038/299126a0

Berghs, S., Aggujaro, D., Dirx, R., Maksimova, E., Stabach, P., Hermel, J. M., Zhang, J. P., Philbrick, W., Slepnev, V., Ort, T. et al. (2000). betaIV spectrin, a new spectrin localized at axon initial segments and nodes of ranvier in the central and peripheral nervous system. *J. Cell Biol.* **151**, 985-1002. doi:10.1083/jcb.151.5.985

Betz, T., Lenz, M., Joanny, J.-F. and Sykes, C. (2009). ATP-dependent mechanics of red blood cells. *Proc. Natl. Acad. Sci. U. S. A.* **106**, 15320-15325. doi:10.1073/pnas.0904614106

Brown, J. W., Bullitt, E., Sriswasdi, S., Harper, S., Speicher, D. W. and McKnight, C. J. (2015). The physiological molecular shape of spectrin: a compact supercoil resembling a chinese finger trap. *PLOS Comput. Biol.* **11**, e1004302. doi:10.1371/journal.pcbi.1004302

Burridge, K., Kelly, T. and Mangeat, P. (1982). Nonerythrocyte spectrins: actin-membrane attachment proteins occurring in many cell types. *J. Cell Biol.* **95**, 478-486. doi:10.1083/jcb.95.2.478

Bustamante, C., Marko, J. F., Siggia, E. D. and Smith, S. (1994). Entropic elasticity of  $\lambda$ -Phage DNA. *Science* **265**, 1599-1600. doi:10.1126/science.8079175

Byers, T. J. and Branton, D. (1985). Visualization of the protein associations in the erythrocyte membrane skeleton. *Proc. Natl. Acad. Sci. U. S. A.* **82**, 6153-6157. doi:10.1073/pnas.82.18.6153

Canham, P. B. (1970). The minimum energy of bending as a possible explanation of the biconcave shape of the human red blood cell. *J. Theor. Biol.* **26**, 61-81. doi:10.1016/S0022-5193(70)80032-7

Cohen, C. M., Tyler, J. M. and Branton, D. (1980). Spectrin-actin associations studied by electron microscopy of shadowed preparations. *Cell* **21**, 875-883. doi:10.1016/0092-8674(80)90451-1

Costa, A. R., Sousa, S. C., Pinto-Costa, R., Mateus, J. C., Lopes, C. D., Costa, A. C., Rosa, D., Machado, D., Pajuelo, L., Wang, X. et al. (2020). The membrane periodic skeleton is an actomyosin network that regulates axonal diameter and conduction. *eLife* **9**, e55471. doi:10.7554/eLife.55471

Cousin, M. A., Creighton, B. A., Breaux, K. A., Spillmann, R. C., Torti, E., Dontu, S., Tripathi, S., Ajit, D., Edwards, R. J., Afriyie, S. et al. (2021). Pathogenic SPTBN1 variants cause an autosomal dominant neurodevelopmental syndrome. *Nat. Genet.* **53**, 1006-1021. doi:10.1038/s41588-021-00886-z

DeSilva, T. M., Harper, S. L., Kotula, L., Hensley, P., Curtis, P. J., Otvos, L. and Speicher, D. W. (1997). Physical properties of a single-motif erythrocyte spectrin peptide: a highly stable independently folding unit. *Biochemistry* **36**, 3991-3997. doi:10.1021/bi962412j

D'Este, E., Kamin, D., Velte, C., Göttfert, F., Simons, M. and Hell, S. W. (2016). Subcortical cytoskeleton periodicity throughout the nervous system. *Sci. Rep.* **6**, 22741. doi:10.1038/srep22741

Dubey, S., Bhembre, N., Bodas, S., Veer, S., Ghose, A., Callan-Jones, A. and Pullarkat, P. (2020). The axonal actin-spectrin lattice acts as a tension buffering shock absorber. *eLife* **9**, e51772. doi:10.7554/eLife.51772

Dupire, J., Socol, M. and Viallat, A. (2012). Full dynamics of a red blood cell in shear flow. *Proc. Natl. Acad. Sci.* **109**, 20808-20813. doi:10.1073/pnas.1210236109

Elgsaeter, A., Stokke, B. T., Mikkelsen, A. and Branton, D. (1986). The molecular basis of erythrocyte shape. *Science* **234**, 1217-1223. doi:10.1126/science.3775380

Evans, E. and Ritchie, K. (1997). Dynamic strength of molecular adhesion bonds. *Biophys. J.* **72**, 1541-1555. doi:10.1016/S0006-3495(97)78802-7

Fowler, V. M. (2013). The human erythrocyte plasma membrane: a Rosetta Stone for decoding membrane-cytoskeleton structure. *Curr. Top. Membr.* **72**, 39-88. doi:10.1016/B978-0-12-417027-8.00002-7

Geekiyana, N. M., Balanant, M. A., Sauret, E., Saha, S., Flower, R., Lim, C. T. and Gu, Y. (2019). A coarse-grained red blood cell membrane model to study stomatocyte-discocyte-echinocyte morphologies. *PLOS ONE* **14**, e0215447. doi:10.1371/journal.pone.0215447

Glennay, J. R., Glennay, P. and Weber, K. (1982). F-actin-binding and cross-linking properties of porcine brain fodrin, a spectrin-related molecule. *J. Biol. Chem.* **257**, 9781-9787. doi:10.1016/S0021-9258(18)34140-1

Gokhin, D. S. and Fowler, V. M. (2016). Feisty filaments: actin dynamics in the red blood cell membrane skeleton. *Curr. Opin. Hematol.* **23**, 206-214. doi:10.1097/MOH.0000000000000227



- Gokhin, D. S., Nowak, R. B., Khoory, J. A., Piedra, A. de la, Ghiran, I. C. and Fowler, V. M.** (2015). Dynamic actin filaments control the mechanical behavior of the human red blood cell membrane. *Mol. Biol. Cell* **26**, 1699-1710. doi:10.1091/mbc.E14-12-1583
- Goodman, S. R., Zagon, I. S. and Kulikowski, R. R.** (1981). Identification of a spectrin-like protein in nonerythroid cells. *Proc. Natl. Acad. Sci. U. S. A.* **78**, 7570-7574. doi:10.1073/pnas.78.12.7570
- Gov, N. S.** (2007). Active elastic network: cytoskeleton of the red blood cell. *Phys. Rev. E Stat. Nonlin. Soft Matter Phys.* **75**, 011921. doi:10.1103/PhysRevE.75.011921
- Grum, V. L., Li, D., MacDonald, R. I. and Mondragón, A.** (1999). Structures of two repeats of spectrin suggest models of flexibility. *Cell* **98**, 523-535. doi:10.1016/S0092-8674(00)81980-7
- Hammarlund, M., Jorgensen, E. M. and Bastiani, M. J.** (2007). Axons break in animals lacking  $\beta$ -spectrin. *J. Cell Biol.* **176**, 269. doi:10.1083/jcb.200611117
- Han, B., Zhou, R., Xia, C. and Zhuang, X.** (2017). Structural organization of the actin-spectrin-based membrane skeleton in dendrites and soma of neurons. *Proc. Natl. Acad. Sci. U. S. A.* **114**, E6678-E6685. doi:10.1073/pnas.1705043114
- Hauser, M., Yan, R., Li, W., Repina, N. A., Schaffer, D. V. and Xu, K.** (2018). The spectrin-actin-based periodic cytoskeleton as a conserved nanoscale scaffold and ruler of the neural stem cell lineage. *Cell Rep.* **24**, 1512-1522. doi:10.1016/j.celrep.2018.07.005
- He, J., Zhou, R., Wu, Z., Carrasco, M. A., Kurshan, P. T., Farley, J. E., Simon, D. J., Wang, G., Han, B., Hao, J. et al.** (2016). Prevalent presence of periodic actin-spectrin-based membrane skeleton in a broad range of neuronal cell types and animal species. *Proc. Natl. Acad. Sci.* **113**, 6029-6034. doi:10.1073/pnas.1605707113
- Hénon, S., Lenormand, G., Richert, A. and Gallet, F.** (1999). A new determination of the shear modulus of the human erythrocyte membrane using optical tweezers. *Biophys. J.* **76**, 1145-1151. doi:10.1016/S0006-3495(99)77279-6
- Huang, C. Y.-M., Zhang, C., Ho, T. S.-Y., Osés-Prieto, J., Burlingame, A. L., Lalonde, J., Noebels, J. L., Leterrier, C. and Rasband, M. N.** (2017a).  $\alpha$ II Spectrin forms a periodic cytoskeleton at the axon initial segment and is required for nervous system function. *J. Neurosci. Off. J. Soc. Neurosci.* **37**, 11311-11322. doi:10.1523/JNEUROSCI.2112-17.2017
- Huang, C. Y.-M., Zhang, C., Zollinger, D. R., Leterrier, C. and Rasband, M. N.** (2017b). An  $\alpha$ II spectrin-based cytoskeleton protects large-diameter myelinated axons from degeneration. *J. Neurosci. Off. J. Soc. Neurosci.* **37**, 11323-11334. doi:10.1523/JNEUROSCI.2113-17.2017
- Jia, R., Li, D., Li, M., Chai, Y., Liu, Y., Xie, Z., Shao, W., Xie, C., Li, L., Huang, X. et al.** (2019). Spectrin-based membrane skeleton supports ciliogenesis. *PLoS Biol.* **17**, e3000369. doi:10.1371/journal.pbio.3000369
- Johnson, C. P., Tang, H.-Y., Carag, C., Speicher, D. W. and Discher, D. E.** (2007). Forced unfolding of proteins within cells. *Science* **317**, 663-666. doi:10.1126/science.1139857
- Kant, A., Johnson, V. E., Arena, J. D., Dollé, J.-P., Smith, D. H. and Shenoy, V. B.** (2021). Modeling links softening of myelin and spectrin scaffolds of axons after a concussion to increased vulnerability to repeated injuries. *Proc. Natl. Acad. Sci. USA* **118**, e2024961118. doi:10.1073/pnas.2024961118
- Kellermayer, M. S. Z., Smith, S. B., Granzier, H. L. and Bustamante, C.** (1997). Folding-unfolding transitions in single titin molecules characterized with laser tweezers. *Science* **276**, 1112-1116. doi:10.1126/science.276.5315.1112
- Kevenaar, J. T. and Hoogenraad, C. C.** (2015). The axonal cytoskeleton: from organization to function. *Front. Mol. Neurosci.* **8**, 44. doi:10.3389/fnmol.2015.00044
- Kim, J., Lee, H. and Shin, S.** (2015). Advances in the measurement of red blood cell deformability: a brief review. *J. Cell. Biotechnol.* **1**, 63-79. doi:10.3233/JCB-15007
- Krieg, M., Dunn, A. R. and Goodman, M. B.** (2014). Mechanical control of the sense of touch by  $\beta$ -spectrin. *Nat. Cell Biol.* **16**, 224-233. doi:10.1038/ncb2915
- Krieger, C. C., An, X., Tang, H.-Y., Mohandas, N., Speicher, D. W. and Discher, D. E.** (2011). Cysteine shotgun-mass spectrometry (CS-MS) reveals dynamic sequence of protein structure changes within mutant and stressed cells. *Proc. Natl. Acad. Sci. USA* **108**, 8269-8274. doi:10.1073/pnas.1018887108
- Kusunoki, H., MacDonald, R. I. and Mondragón, A.** (2004). Structural insights into the stability and flexibility of unusual erythroid spectrin repeats. *Struct. Lond. Engl.* **12**, 645-656.
- Law, R., Carl, P., Harper, S., Dalhaimer, P., Speicher, D. W. and Discher, D. E.** (2003). Cooperativity in forced unfolding of tandem spectrin repeats. *Biophys. J.* **84**, 533-544. doi:10.1016/S0006-3495(03)74872-3
- Lee, J. C.-M. and Discher, D. E.** (2001). Deformation-enhanced fluctuations in the red cell skeleton with theoretical relations to elasticity, connectivity, and spectrin unfolding. *Biophys. J.* **81**, 3178-3192. doi:10.1016/S0006-3495(01)75954-1
- Leite, S. C., Sampaio, P., Sousa, V. F., Nogueira-Rodrigues, J., Pinto-Costa, R., Peters, L. L., Brites, P. and Sousa, M. M.** (2016). The actin-binding protein  $\alpha$ -adducin is required for maintaining axon diameter. *Cell Rep.* **15**, 490-498. doi:10.1016/j.celrep.2016.03.047
- Leterrier, C.** (2021). Putting the axonal periodic scaffold in order. *Curr. Opin. Neurobiol.* **69**, 33-40. doi:10.1016/j.conb.2020.12.015
- Leterrier, C., Dubey, P. and Roy, S.** (2017). The nano-architecture of the axonal cytoskeleton. *Nat. Rev. Neurosci.* **18**, 713-726. doi:10.1038/nrn.2017.129
- Levine, J. and Willard, M.** (1981). Fodrin: axonally transported polypeptides associated with the internal periphery of many cells. *J. Cell Biol.* **90**, 631-642. doi:10.1083/jcb.90.3.631
- Li, H., Lu, L., Li, X., Buffet, P. A., Dao, M., Karniadakis, G. E. and Suresh, S.** (2018). Mechanics of diseased red blood cells in human spleen and consequences for hereditary blood disorders. *Proc. Natl. Acad. Sci. U. S. A.* **115**, 9574-9579. doi:10.1073/pnas.1806501115
- Liu, C.-H. and Rasband, M. N.** (2019). Axonal spectrins: nanoscale organization, functional domains and spectrinopathies. *Front. Cell. Neurosci.* **13**, 234. doi:10.3389/fncel.2019.00234
- Liu, S. C., Derick, L. H. and Palek, J.** (1987). Visualization of the hexagonal lattice in the erythrocyte membrane skeleton. *J. Cell Biol.* **104**, 527-536. doi:10.1083/jcb.104.3.527
- Liu, Y., Qi, J., Chen, X., Tang, M., Chu, C., Zhu, W., Li, H., Tian, C., Yang, G., Zhong, C. et al.** (2019). Critical role of spectrin in hearing development and deafness. *Sci. Adv.* **5**, eaav7803. doi:10.1126/sciadv.aav7803
- Lorenzo, D. N.** (2020). Cargo hold and delivery: Ankyrins, spectrins, and their functional patterning of neurons. *Cytoskeleton* **77**, 129-148. doi:10.1002/cm.21602
- Lux, S. E., IV** (2016). Anatomy of the red cell membrane skeleton: unanswered questions. *Blood* **127**, 187-199. doi:10.1182/blood-2014-12-512772
- Machnicka, B., Czogalla, A., Hryniewicz-Jankowska, A., Bogusławska, D. M., Grochowalska, R., Heger, E. and Sikorski, A. F.** (2014). Spectrins: a structural platform for stabilization and activation of membrane channels, receptors and transporters. *Biochim. Biophys. Acta* **1838**, 620-634. doi:10.1016/j.bbamem.2013.05.002
- Marchesi, V. T. and Steers, E.** (1968). Selective solubilization of a protein component of the red cell membrane. *Science* **159**, 203-204. doi:10.1126/science.159.3811.203
- McGough, A. M. and Josephs, R.** (1990). On the structure of erythrocyte spectrin in partially expanded membrane skeletons. *Proc. Natl. Acad. Sci. U. S. A.* **87**, 5208-5212. doi:10.1073/pnas.87.13.5208
- Mills, J. P., Qie, L., Dao, M., Lim, C. T. and Suresh, S.** (2004). Nonlinear elastic and viscoelastic deformation of the human red blood cell with optical tweezers. *Mech. Chem. Biosyst. MCB* **1**, 169-180.
- Mohandas, N. and Evans, E.** (1994). Mechanical properties of the red cell membrane in relation to molecular structure and genetic defects. *Annu. Rev. Biophys. Biomol. Struct.* **23**, 787-818. doi:10.1146/annurev.bb.23.060194.004035
- Mutalik, S. P., Joseph, J., Pullarkat, P. A. and Ghose, A.** (2018). Cytoskeletal mechanisms of axonal contractility. *Biophys. J.* **115**, 713-724. doi:10.1016/j.bpj.2018.07.007
- Nans, A., Mohandas, N. and Stokes, D. L.** (2011). Native ultrastructure of the red cell cytoskeleton by Cryo-electron tomography. *Biophys. J.* **101**, 2341-2350. doi:10.1016/j.bpj.2011.09.050
- Nowak, R. B., Alimohamadi, H., Pestonjamas, K., Rangamani, P. and Fowler, V. M.** (2022). Nanoscale dynamics of actin filaments in the red blood cell membrane skeleton. *Mol. Biol. Cell* **33**, ar28. doi:10.1091/mbc.E21-03-0107
- Ohara, O., Ohara, R., Yamakawa, H., Nakajima, D. and Nakayama, M.** (1998). Characterization of a new beta-spectrin gene which is predominantly expressed in brain. *Brain Res. Mol. Brain Res.* **57**, 181-192. doi:10.1016/S0169-328X(98)00068-0
- Ohno, S.** (1992). An ultrastructural study of the cytoplasmic aspects of erythrocyte membranes by a quick-freezing and deep-etching method. *J. Anat.* **180**, 315-320.
- Ortiz, V., Nielsen, S. O., Klein, M. L. and Discher, D. E.** (2005). Unfolding a linker between helical repeats. *J. Mol. Biol.* **349**, 638-647. doi:10.1016/j.jmb.2005.03.086
- Pan, L., Yan, R., Li, W. and Xu, K.** (2018). Super-resolution microscopy reveals the native ultrastructure of the erythrocyte cytoskeleton. *Cell Rep.* **22**, 1151-1158. doi:10.1016/j.celrep.2017.12.107
- Pan, X., Zhou, Y., Hotulainen, P., Meunier, F. A. and Wang, T.** (2021). The axonal radial contractility: structural basis underlying a new form of neural plasticity. *BioEssays News Rev. Mol. Cell. Dev. Biol.* **43**, e2100033. doi:10.1002/bies.202100033
- Prokop, A.** (2020). Cytoskeletal organization of axons in vertebrates and invertebrates. *J. Cell Biol.* **219**, e201912081. doi:10.1083/jcb.201912081
- Pullarkat, P. A., Fernández, P. A. and Ott, A.** (2007). Rheological properties of the Eukaryotic cell cytoskeleton. *Phys. Rep.* **449**, 29-53. doi:10.1016/j.physrep.2007.03.002
- Qu, Y., Hahn, I., Webb, S. E. D., Pearce, S. P. and Prokop, A.** (2017). Periodic actin structures in neuronal axons are required to maintain microtubules. *Mol. Biol. Cell* **28**, 296-308. doi:10.1091/mbc.e16-10-0727
- Rajagopalan, J., Tofangchi, A. and Saif, M. T.** (2010). Drosophila neurons actively regulate axonal tension In Vivo. *Biophys. J.* **99**, 3208-3215. doi:10.1016/j.bpj.2010.09.029
- Randles, L. G., Rounsevell, R. W. S. and Clarke, J.** (2007). Spectrin domains lose cooperativity in forced unfolding. *Biophys. J.* **92**, 571-577. doi:10.1529/biophysj.106.093690

- Repasky, E. A., Granger, B. L. and Lazarides, E.** (1982). Widespread occurrence of avian spectrin in nonerythroid cells. *Cell* **29**, 821-833. doi:10.1016/0092-8674(82)90444-5
- Rief, M., Gautel, M., Oesterhelt, F., Fernandez, J. M. and Gaub, H. E.** (1997). Reversible unfolding of individual titin immunoglobulin domains by AFM. *Science* **276**, 1109-1112. doi:10.1126/science.276.5315.1109
- Rief, M., Pascual, J., Saraste, M. and Gaub, H. E.** (1999). Single molecule force spectroscopy of spectrin repeats: low unfolding forces in helix bundles. *J. Mol. Biol.* **286**, 553-561. doi:10.1006/jmbi.1998.2466
- Seifert, U.** (1997). Configurations of fluid membranes and vesicles. *Adv. Phys.* **46**, 13-137. doi:10.1080/00018739700101488
- Shotton, D. M., Burke, B. E. and Branton, D.** (1979). The molecular structure of human erythrocyte spectrin: biophysical and electron microscopic studies. *J. Mol. Biol.* **131**, 303-329. doi:10.1016/0022-2836(79)90078-0
- Smith, A. S., Nowak, R. B., Zhou, S., Giannetto, M., Gokhin, D. S., Papoin, J., Ghiran, I. C., Blanc, L., Wan, J. and Fowler, V. M.** (2018). Myosin IIA interacts with the spectrin-actin membrane skeleton to control red blood cell membrane curvature and deformability. *Proc. Natl. Acad. Sci.* **115**, E4377-E4385. doi:10.1073/pnas.1718285115
- Speicher, D. W. and Marchesi, V. T.** (1984). Erythrocyte spectrin is comprised of many homologous triple helical segments. *Nature* **311**, 177-180. doi:10.1038/311177a0
- Sreeja, J. S., John, R., Dharmapal, D., Nellikka, R. K. and Sengupta, S.** (2020). A fresh look at the structure, regulation, and functions of fodrin. *Mol. Cell. Biol.* **40**, e00133-e00120. doi:10.1128/MCB.00133-20
- Stabach, P. R. and Morrow, J. S.** (2000). Identification and characterization of beta V spectrin, a mammalian ortholog of Drosophila beta H spectrin. *J. Biol. Chem.* **275**, 21385-21395. doi:10.1074/jbc.C000159200
- Stokke, B. T., Mikkelsen, A. and Elgsaeter, A.** (1985). Human erythrocyte spectrin dimer intrinsic viscosity: temperature dependence and implications for the molecular basis of the erythrocyte membrane free energy. *Biochim. Biophys. Acta* **816**, 102-110. doi:10.1016/0005-2736(85)90398-0
- Storm, C., Pastore, J. J., MacKintosh, F. C., Lubensky, T. C. and Janmey, P. A.** (2005). Nonlinear elasticity in biological gels. *Nature* **435**, 191-194. doi:10.1038/nature03521
- Tomaiuolo, G.** (2014). Biomechanical properties of red blood cells in health and disease towards microfluidics. *Biomicrofluidics* **8**, 051501. doi:10.1063/1.4895755
- Tsukita, S., Tsukita, S., Ishikawa, H., Sato, S. and Nakao, M.** (1981). Electron microscopic study of reassociation of spectrin and actin with the human erythrocyte membrane. *J. Cell Biol.* **90**, 70-77. doi:10.1083/jcb.90.1.70
- Ursitti, J. A. and Fowler, V. M.** (1994). Immunolocalization of tropomodulin, tropomyosin and actin in spread human erythrocyte skeletons. *J. Cell Sci.* **107**, 1633-1639. doi:10.1242/jcs.107.6.1633
- Wang, T., Li, W., Martin, S., Papadopoulos, A., Joensuu, M., Liu, C., Jiang, A., Shamsollahi, G., Amor, R., Lanoue, V. et al.** (2020). Radial contractility of actomyosin rings facilitates axonal trafficking and structural stability. *J. Cell Biol.* **219**, e201902001. doi:10.1083/jcb.201902001
- Wasenius, V. M., Saraste, M., Salvén, P., Erämaa, M., Holm, L. and Lehto, V. P.** (1989). Primary structure of the brain alpha-spectrin. *J. Cell Biol.* **108**, 79-93. doi:10.1083/jcb.108.1.79
- Waugh, R. and Evans, E. A.** (1979). Thermoelasticity of red blood cell membrane. *Biophys. J.* **26**, 115-131. doi:10.1016/S0006-3495(79)85239-X
- Winkelmann, J. C. and Forget, B. G.** (1993). Erythroid and nonerythroid spectrins. *Blood* **81**, 3173-3185. doi:10.1182/blood.V81.12.3173.3173
- Xu, K., Zhong, G. and Zhuang, X.** (2013). Actin, spectrin and associated proteins form a periodic cytoskeletal structure in axons. *Science* **339**, 452-456. doi:10.1126/science.1232251
- Yao, M., Goult, B. T., Klapholz, B., Hu, X., Toseland, C. P., Guo, Y., Cong, P., Sheetz, M. P. and Yan, J.** (2016). The mechanical response of talin. *Nat. Commun.* **7**, 11966. doi:10.1038/ncomms11966
- Zhang, Y., Abiraman, K., Li, H., Pierce, D. M., Tzingounis, A. V. and Lykotrafitis, G.** (2017). Modeling of the axon membrane skeleton structure and implications for its mechanical properties. *PLOS Comput. Biol.* **13**, e1005407. doi:10.1371/journal.pcbi.1005407
- Zhou, R., Han, B., Xia, C. and Zhuang, X.** (2019). Membrane-associated periodic skeleton is a signaling platform for RTK transactivation in neurons. *Science* **365**, 929-934. doi:10.1126/science.aaw5937